

# Sorting of bending magnets for the SSRF booster<sup>\*</sup>

HOU Jie(后接)<sup>1,2</sup> LIU Gui-Min(刘桂民)<sup>1,1)</sup> LI Hao-Hu(李浩虎)<sup>1</sup> ZHANG Man-Zhou(张满洲)<sup>1,2</sup>

<sup>1</sup> (Shanghai Institute of Applied Physics, CAS, Shanghai 201800, China)

<sup>2</sup> (Graduate University of Chinese Academy of Sciences, Beijing 100049, China)

**Abstract** The Shanghai Synchrotron Radiation Facility (SSRF) booster ring, a full energy injector for the storage ring, is deigned to accelerate the electron beam energy from 150 MeV to 3.5 GeV that demands high extraction efficiency at the extraction energy with low beam loss rate when electrons are ramping. Closed orbit distortion (COD) caused by bending magnet field uniformity errors which affects the machine performance harmfully could be effectively reduced by bending magnet location sorting. Considering the affections of random errors in measurement, both ideal sorting and realistic sorting are studied based on measured bending magnet field uniformity errors and one reasonable combination of bending magnets which can reduce the horizontal COD by a factor of 5 is given as the final installation sequence of the booster bending magnets in this paper.

**Key words** SSRF, bending magnet, sorting, uniformity, resolution

**PACS** 29.20.D-, 29.25.Bx

## 1 Introduction

The SSRF booster lattice, 180 m in circumference, is a two-fold symmetry and 28-FODO-cell structure comprising 48 bending magnets and 8 straight sections<sup>[1]</sup>. The magnets layouts are the same in two superperiods and symmetric inside one superperiod, one standard cell layout is shown in Fig. 1. As the bending magnets are not laid in the centre of the space between the focusing and defocusing quadrupoles (QF&QD) in each cell, and the sizes of the QF and QD are different, there are 4 types of girders on which the bending magnets are firstly installed and pre-aligned. Table 1 shows the detail.

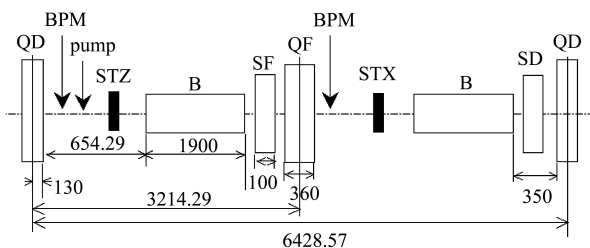


Fig. 1. Layout showing bending (B), quadrupole (QF, QD), sextupole (SF,SD), and corrector (STX,STZ) magnets of one cell.

COD in the booster mainly comes from the bending magnet field uniformity errors (field error for short) and quadrupole misalignment. Large COD usually affects the booster ring performance: (1) decreases the injection efficiency at injection energy, (2) reduces the beam extraction efficiency at extraction energy, and makes the beam extraction difficult to some extent, and (3) induces large beam loss during the electron beam ramping.

Table 1. Booster girder type and magnets installed.

girder type	girder position	magnets installed	No. of bending magnets
A	1st, 3rd quadrant	QF+SF+B	14(2)*
B	1st, 3rd quadrant	QD+SD+B	10
C	2nd, 4th quadrant	B+SF+QF	14(3)
D	2nd, 4th quadrant	B+SD+QD	10(1)

\* No. in bracket indicates the No. of restricted bending magnets.

COD at injection energy can be corrected by using 28 static correctors in both the horizontal and vertical planes. But COD at extraction energy still needs correction because the currents of correctors are not varied with the electron beam ramping. There are two active ways to solve this problem. One is the bending magnet location sorting (sorting for short) by their field errors, the other one is to control the roof mean

Received 13 June 2007

\* Supported by SSRF Project

1) E-mail: liugm@sinap.ac.cn

square (rms) transverse misalignment of quadrupoles strictly below 0.15 mm to ensure the rms COD below 2 mm in the horizontal and vertical planes<sup>[1]</sup>. In this paper, we mainly study sorting at extraction energy which is necessary and practicable to reduce the horizontal COD caused by field errors by a factor of 5.

Bending magnet field errors, creating COD in the horizontal plane, can be regarded as small horizontal correctors, so sorting can be treated as the horizontal COD correction. The horizontal COD could be effectively reduced when the number of correctors is larger than  $4\nu_x$  (horizontal betatron tune). In the SSRF booster, 6 bending magnets are pre-restricted in the tunnel because the vacuum chambers inside these bending magnets are different from the others. (B1900-12 and B1900-19 is pre-restricted at the 1st and 48th bending magnet location for injection while B1900-34, -40, -41, -9 are pre-restricted at the 20th, 23th, 24th, 25th bending magnet location for extraction). The number of bending magnets to be sorted in fact, 42, is still larger than  $4\nu_x$  which is nearly 32 as the SSRF Booster works at [8.181, 5.229]. As the number of bending magnets to be sorted is adequate, the horizontal COD after the realistic sorting, in which case bending magnets can only be exchanged within the same types of girder, will be close to ideal sorting, in which case the bending magnets can be exchanged without any limitations. Since the bending magnets are already installed on girders during measurement, the realistic sorting will also save the project workload, as the bending magnets need to be re-installed and re-measured when they are in exchange with different types of girders.

The bending magnets are sorted in the SNS ring according to the following rule: (1) Pairing out of range bending magnets, (2) place two bending magnets of equal errors  $\pi$  radians apart in phase for cancellation, (3) or place two bending magnets with opposite errors  $2\pi$  radians apart<sup>[2]</sup>. By sorting pairs of bending magnets having the closest simulated measured field errors, the driving term of the integer resonance nearest the operating point of COD is reduced in the APS injector synchrotron<sup>[3, 4]</sup>. In our case, the bending magnets are firstly ranked by the absolute value of field errors from large to small, then placed at the location, found by simulation which minimizes the COD at each step, one by one.

## 2 Sorting method

### 2.1 Bending magnets field measurement

The peak field of bending magnets in design is 0.035 T at 150 MeV and 0.804 T at 3.5 GeV. The

coils (each bending magnet contains two independent ones) are powered crossed in series by two independent power supplies so that the peak voltage of each power supply can be reduced to 868 V which is available according to the electrical safety standards<sup>[5]</sup>. The field error for each bending magnet is defined as:

$$\frac{\Delta(BL)}{(BL)} \Big|_i = \frac{(BL)_i - (BL)_a}{(BL)_a}, \quad (1)$$

where  $(BL)_a$  is the average bending magnet integral field strength while  $(BL)_i$  is that of  $i$ th one at the rated excitation current.

The B1900-24 is selected as the reference bending magnet during the field measurement. The integral field strengths of each bending magnet at different currents are measured and the values of them are given by the ratio compared to that of the reference magnet which is also measured in one measurement process. The excitation current varies from 10 A to 980 A in a step of 10 A for every measurement. Fig. 2 shows the measured field errors of each bending magnet at 980 A, the rms field errors is  $6 \times 10^{-4}$ .

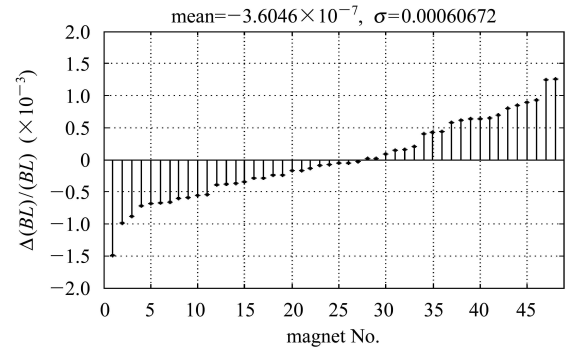


Fig. 2. Bending magnet field errors at 980 A.

### 2.2 Resolution of measurement

Errors exist during the measurement. The resolution of measurement  $\sigma$  can be defined by measuring the bending magnet many times one by one:

$$\sigma = \sqrt{\frac{\sum_{i=1}^m \sum_{j=1}^n \Delta_{i,j}^2}{mn - 1}}, \quad (2)$$

where  $m$  is the number of measured bending magnets and  $n$  is the measurement times for every bending magnet, and  $\Delta_{i,j}$  is the difference between the  $j$ th measured value and the average value of integral field strength for  $i$ th bending magnet. As the integral field strength for each bending magnet is twice repetitively measured and the resolution of measuring one bending magnet many times is the same as measuring different bending magnets repeatedly, we adopt the relative error of repeated measurements in rms as approximate resolution of measurement.

Since the integral field strength is given in ratio comparing to the reference magnet, both the target and the reference bending magnet are measured in one measurement process. The system error of measurement, arising from temperature drift and other change of measurement environment, is reduced effectively. The measurement result is more accurate. Fig. 3 shows the resolution of measurement,  $3.3 \times 10^{-5}$  which is about 1/20 of the rms field errors, at 980 A.

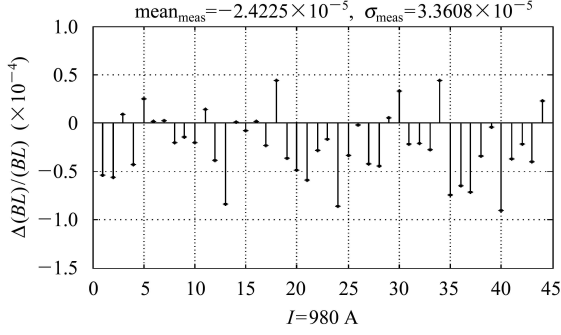


Fig. 3. Resolution of measurement at 980 A.

A measured value of field error comprises two parts: the systematic value and the random one. We can only judge the effect of sorting by using systematic values in sorting. And how much the realistic COD differs from the simulation result is determined by the random values. For processing the sorting by systematic field errors, the bending magnets are grouped based on the measured field errors as follows. The difference between the maximal and minimal field errors at 980 A is  $2.75 \times 10^{-3}$ , adopting the class interval three times of the resolution of measurement as  $1 \times 10^{-4}$ . So the number of groups, decided by the quotient as the field errors difference divided by the class interval, is selected as 28. The field errors of each bending magnet, which are the same in one bending magnet group, are used as systematic field errors when sorting processes as shown in Fig. 4. The number of bending magnets in each group by realistic sorting is shown in Table 2.

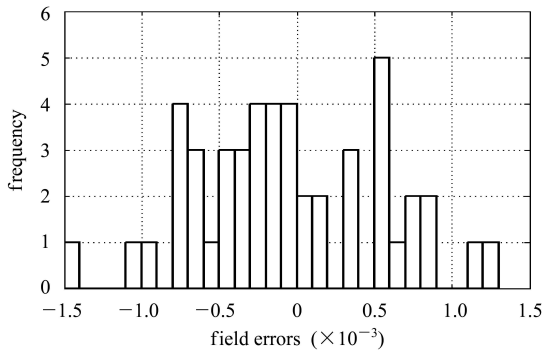


Fig. 4. Distribution of field errors after grouping at 980 A.

Table 2. Grouping of bending magnets in realistic sorting.

girder type	group No.	total bending magnet No.	bending magnet No. in each group
A	8	12	1/2/1/1/4/1/1/1
B	6	10	4/2/1/1/1/1
C	10	11	1/1/1/1/1/2/1/1/1/1
D	7	9	1/1/2/1/1/1/2

## 2.3 Sorting method

The contribution to horizontal COD by the bending magnet field errors is determined as:

$$x_{\text{COD}} = \frac{\sqrt{\beta}}{2 \sin \pi \nu} \sum_{i=1}^N \theta_{\Delta B/B_i} \sqrt{\beta_i} \cos(\pi \nu - \Delta \psi), \quad (3)$$

where  $\beta$  and  $\beta_i$  are the  $\beta$  function of observation point and error source,  $\Delta \psi$  is the phase advance from the error source to the observation point,  $N$  is the number of bending magnets, and  $\theta_{\Delta B/B_i}$  is the kick by the  $i$ th bending magnet field error. Both rms and the peak value of COD are considered in the object function to get better result by choosing proper weight  $\alpha$ :

$$f = \text{COD}_{\text{rms}} + \alpha |\text{COD}_{\text{peak}}|. \quad (4)$$

A simple way of sorting is to find out the combination which minimizes the object function in all possible combinations. The number of possible combinations grown as  $N!$ , where  $N$  is the number of bending magnets, is astronomical and impossible to be enumerated as the time complexity of codes in simulation which generates all possible combinations is  $O(N!)$ . For the SSRF Booster, the number of combinations for ideal sorting is  $48!$  which equals  $1.24 \times 10^{61}$ . Since 6 bending magnets are pre-restricted in the tunnel and the systematic field errors are the same in each group, the number of possible combinations for realistic sorting is greatly reduced, but it still remains:

$$\frac{12!}{1!2!1!1!4!1!1!1!} \times \frac{10!}{4!2!1!1!1!1!} \times \frac{11!}{1!1!1!1!1!2!1!1!1!1!} \times \frac{9!}{1!1!2!1!1!1!2!} = 1.37 \times 10^{24}. \quad (5)$$

The possible combinations for ideal and realistic sorting are too difficult to be enumerated.

By choosing proper phase advance  $\psi$ , the contribution of two bending magnet field errors to the horizontal COD can be cancelled and suitable combinations could be found: selecting two bending magnets whose values of field errors are opposite and place them in the tunnel while  $\Delta \psi \approx k\pi \nu$  ( $k$  is even); pairing off two bending magnets whose values of field errors are equal while  $\Delta \psi \approx k\pi \nu$  ( $k$  is odd).

In our case, COD is cancelled by finding the proper bending magnet location, i.e. finding proper phase advance, which minimizes the COD at each

step in simulation. The sorting process is shown as below: (1) firstly place the bending magnet whose absolute value of field error is the largest to the location whose object function is the minimum one among all the locations that could be placed, (2) place the bending magnet of the second absolute value in field error where the object function is the minimum one among all the locations which remain to be placed, and (3) follow the step above to place the bending magnets by the ranking of the absolute value of the field errors from large to small one by one. The time complexity of codes in our simulation is  $O(N^2)$ . A

suitable combination can be found quickly. COD is determined by AT<sup>[6]</sup> based on MATLAB.

### 3 Results of sorting

Without sorting, the horizontal COD caused by 1000 random combinations of bending magnet field errors are shown as follows: (1) COD in rms from 0.394 mm to 4.327 mm, mostly 1–2 mm, (2) the absolute peak value of COD from 1.178 mm to 9.610 mm, mostly 2–6 mm.

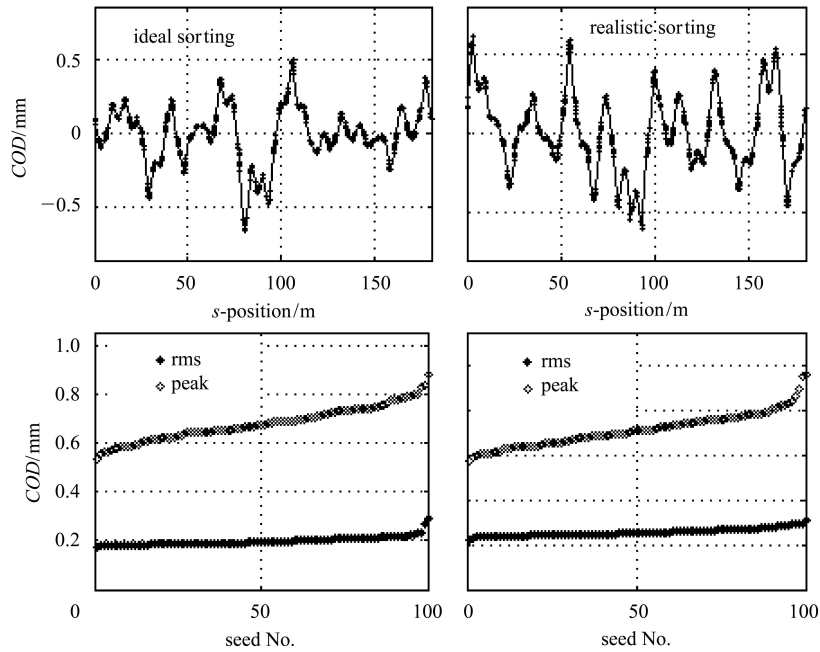


Fig. 5. Results of ideal and realistic sorting.

After sorting, the typical horizontal COD and distribution of horizontal COD with 100 random errors on measurement ( $3\sigma$  cut off) is shown in Fig. 5. The typical horizontal COD is 0.185 mm and 0.243 mm separately in rms after ideal and realistic sorting while the absolute peak value of COD is 0.666 mm and 0.620 mm. With the effects of random errors in measurement, the rms COD varies from 0.176 mm to 0.290 mm and from 0.221 mm to 0.313 mm while the absolute peak value of COD goes from 0.534 mm to 0.882 mm and from 0.575 mm to 0.958 mm after ideal and realistic sorting, respectively. The difference between the CODs after ideal and realistic sorting is small as estimated above.

COD after sorting can be smaller in rms or at peak by choosing proper weight in object function. The effect of the weight choosing on the typical COD after sorting is studied as shown in Fig. 6. The weight are chosen as 0.15 for both of ideal and realistic sorting.

COD after sorting depends on the horizontal be-

tatron tune, as the phase advance between two bending magnets varies with the change of horizontal tune. Adjusting the horizontal tune by tuning the excitation current of QFs, when the bending magnets are

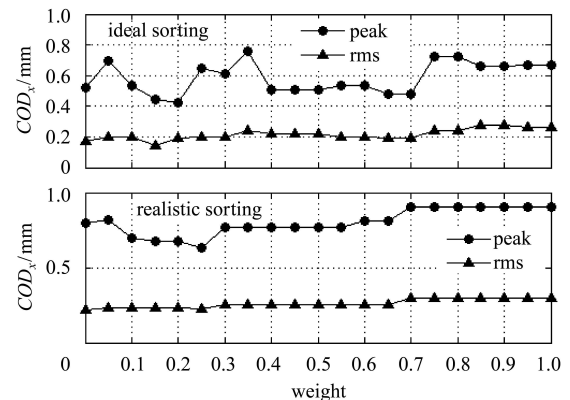


Fig. 6. Affections of weight choosing to COD after sorting.

installed follow the sequence obtained from the realistic sorting. The horizontal COD varies a little when the horizontal tune is changed in decimal part near 8.181. But it will grow rapidly, the rms and the absolute peak value of horizontal COD change from 0.243 mm to 0.485 mm and from 0.620 mm to 1.426 mm separately, while the horizontal tune is changed in integral part from 8.181 to 7.182.

The horizontal COD after realistic sorting is a little worse than that after ideal sorting for the limitation of bending magnet locations, but meets the requirements of optimization. Considering the trade off between horizontal COD after sorting and project workload, finally we install the bending magnets by following the sequence obtained from the realistic sorting as shown in Table 3.

Table 3. Installation sequence of bending magnets.

index	girder type	label of bending magnets	field errors( $\times 10^{-3}$ )	index	girder type	label of bending magnets	field errors( $\times 10^{-3}$ )
1	A	B1900-12	0.6	25	A	B1900-09	-0.5
2	A	B1900-04	0.6	26	A	B1900-05	-0.4
3	B	B1900-43	-0.7	27	B	B1900-28	0.2
4	A	B1900-20	1.3	28	A	B1900-07	0.6
5	B	B1900-31	-0.1	29	B	B1900-01	-0.7
6	A	B1900-21	0.2	30	A	B1900-16	0.8
7	B	B1900-29	-0.6	31	B	B1900-47	-0.7
8	A	B1900-22	0.6	32	A	B1900-15	0.6
9	B	B1900-46	-0.2	33	B	B1900-45	-0.7
10	A	B1900-06	-0.2	34	A	B1900-17	0.9
11	B	B1900-32	0.0	35	B	B1900-49	-0.6
12	A	B1900-03	-0.2	36	A	B1900-02	-0.1
13	C	B1900-08	0.7	37	C	B1900-13	0.4
14	D	B1900-48	-0.1	38	D	B1900-36	-0.3
15	C	B1900-11	0.0	39	C	B1900-42	-0.1
16	D	B1900-14	0.0	40	D	B1900-35	-0.6
17	C	B1900-23	0.8	41	C	B1900-10	0.1
18	D	B1900-30	-0.4	42	D	B1900-33	-0.4
19	C	B1900-27	-0.3	43	C	B1900-37	0.4
20	D	B1900-34	0.4	44	D	B1900-44	-0.2
21	C	B1900-25	-0.9	45	C	B1900-18	1.2
22	D	B1900-38	0.0	46	D	B1900-39	-1.0
23	C	B1900-40	-0.3	47	C	B1900-26	0.9
24	C	B1900-41	-1.5	48	C	B1900-19	0.1

## 4 Conclusions

The measured SSRF booster bending magnet filed error is  $6 \times 10^{-4}$  in rms at 980 A. Sorting yields a reduction factor of 5 in horizontal COD caused by the bending magnet field errors. The horizontal COD af-

ter sorting by the systematic field errors is 0.243 mm in rms and 0.620 mm at peak. With the effects of random errors in measurement which is about 1/20 of the rms field errors, the horizontal COD after sorting is still below 0.3 mm that meets the requirements of bending magnet sorting optimization.

## References

- 1 SSRF Design Report. Chapter 3. 2005
- 2 Raparia D et al. Dipole and Quadrupole Sorting for the SNS Ring, EPAC2004 Conference Proceedings. Lucerne, Switzerland. 2004. 1574
- 3 Koul R K, Lopez F, Mills F E. Optimal Magnet Sorting Procedure and Application to the APS Injector Synchrotron. PAC93 Conference Proceedings. Washington, 1993, 4: 2924
- 4 Lopez F. Effect of Magnet Sorting Using a Simple Resonance Cancellation Method on the rms Orbit Distortion at the APS Injector Synchrotron, PAC93 Conference Proceedings. Washington, 1993, 4: 2922
- 5 SSRF Design Report. Chapter 5. 2005
- 6 Terebilo A. Accelerator Toolbox for MATLAB, SLAC-PUB-8732. <http://www.slac.stanford.edu/~terebedo/at/>